Received: 27 July 2022 | Revised: 8 November 2022 | Accepted: 10 November 2022

DOI: 10.1002/jcla.24781

RESEARCH ARTICLE

WILEY

Hsa_circ_0092887 targeting miR-490-5p/UBE2T promotes paclitaxel resistance in non-small cell lung cancer

Limei Wang[1] | Zhiyong Zhang[1] | Hui Tian[2]

[1]Department of Pharmacy, Wuhan Hospital of Traditional Chinese Medicine, Wuhan, China

[2]Department of Pulmonary Diseases, Wuhan Hospital of Traditional Chinese Medicine, Wuhan, China

Correspondence
Hui Tian, Department of Pulmonary Diseases, Wuhan Hospital of Traditional Chinese Medicine, No. 303 Sixin Avenue, Hanyang, Wuhan 430000, Hubei, China.
Email: tianhui595@163.com

Abstract

Background: Chemoresistance is a major contributing factor to cancer treatment failure. Emerging research reveals that circular RNA (circRNA) dysregulation is implicated in chemoresistance. Our current study aimed to investigate the involvement of hsa_circ_0092887 in paclitaxel (PTX) resistance in non-small cell lung cancer (NSCLC).

Methods: RT-qPCR as well as western blotting were used for the analysis of hsa_circ_0092887, miR-490-5p and UBE2T expression in PTX-resistant NSCLC tumor tissues and cells. CCK-8 assay was done to determine the IC50 value of PTX. CCK-8 assay, wound healing assay, analysis of apoptosis related proteins (Bax and Bcl-2), and xenograft mouse models were utilized to investigate the role of hsa_circ_0092887 in PTX-resistance in NSCLC. The binding sites of miR-490-5p to hsa_circ_0092887 or UBE2T were predicted by bioinformatics tools and were verified by RIP and dual-luciferase assays.

Results: Expression of hsa_Circ_0092887 was upregulated in NSCLC tumor samples/cell lines, and its expression was also higher in PTX-resistant tumor samples/cell lines when compared with their respective controls. Silencing of hsa_circ_0092887 in PTX-treated NSCLC cells inhibited cell proliferation and migration, induced apoptosis, and suppressed tumor growth in xenograft mouse models in vivo. MiR-490-5p was a direct target of hsa_circ_0092887, and UBE2T was a functional downstream target of hsa_circ_0092887/miR-490-5p axis. Hsa_circ_0092887 depletion-induced anti-cancer effects in PTX-treated NSCLC cells were reversed by miR-490-5p inhibitor. Furthermore, inhibition of miR-490-5p strengthened UBE2T expression, thereby attenuating the anti-cancer effects caused by UBE2T knockdown.

Conclusion: Hsa_circ_0092887 depletion alleviated PTX-resistance in NSCLC cells via modulating the miR-490-5p/UBE2T axis, and the targeted management of hsa_circ_0092887-mediated signaling axis might contribute to PTX-resistance intervention in NSCLC.

KEYWORDS
hsa_circ_0092887, miR-490-5p, non-small cell lung cancer, paclitaxel, UBE2T

Limei Wang and Zhiyong Zhang have contributed equally to this study.

1 | INTRODUCTION

Lung cancer is the most prevalent malignant cancer, second only to female breast cancer in terms of global cancer in 2020, and it has the highest mortality rate.[1] The major risk factors for lung cancer are cigarette smoking, asbestos exposure, and air pollution.[2] Non-small cell lung cancer (NSCLC) is the most common type of lung cancer that begins in the lungs. If diagnosed at a late stage, patients may have a shorter survival period (with 25% of 5-year survival).[3] Presently, chemotherapy remains the most important treatment strategy for NSCLC.[4] Paclitaxel (PTX), a chemotherapeutic drug, has a broad spectrum of action against a variety of malignant tumors, and it is the first-line treatment for late-stage NSCLC; nevertheless, the development of PTX-resistance severely limits therapeutic outcomes.[5] Biomarkers are vital for early diagnosis, prediction, and monitoring PTX-resistance.[6,7] Hence, it is crucial to investigate potential biomarkers to manage PTX-resistant NSCLC.

Circular RNAs (circRNAs), which were discovered as non-coding RNAs a few years ago but modern research reveals that they may also act as protein translation templates, have been developed as biomarkers to supplement clinical diagnosis and treatment.[8–10] CircRNAs are well-known for specific closed-loop structures without 5′ and 3′ ends, which confers circRNAs high stabilities. The better understanding of the molecular features related with NSCLC has made it possible to analyze sensitive and specific biomarkers via liquid biopsy,[6] and the use of biomarkers in other types of body fluids or blood for the diagnosis, treatment guidance of NSCLC is becoming increasingly promising.[6] Importantly, circRNAs have been shown to stably exist in multiple body fluids, such as urine, serum, saliva, and exosomes.[11] These characteristics hint that circRNAs, relative to linear molecules, are more promising biomarkers applied in cancer biology. Interestingly, certain circRNAs were reported to be implicated with PTX resistance in NSCLC development. For example, aberrant upregulation of circ_ZFR and circ_0002874 in PTX-resistant NSCLC and depletion of circ_ZFR or circ_0002874 enhanced PTX chemosensitivity and thus blocked PTX-resistant NSCLC cell malignant phenotypes,[12,13] whereas the involvement of several circRNAs in PTX resistance remains unknown. Increasing circRNA expression profiles obtained from RNA-sequencing display that numerous circRNAs are abnormally expressed in NSCLC samples, in contrast to normal samples.[14–16] The data from the GEO dataset GSE112214 revealed that hsa_circ_0092887 is a dysregulated circRNA that is upregulated in NSCLC tissues, which attracted our interest. However, the functional effects of hsa_circ_0092887 on NSCLC development and PTX resistance have not been investigated as yet.

The considerable role of microRNAs (miRNAs) in tumorigenesis and chemoresistance has been widely established. MiR-490-5p has been universally demonstrated as a tumor-suppressor and shows noticeably poor expression in multiple cancers,[17–19] whereas the role of miR-490-5p on chemoresistance is hardly illustrated. Interestingly, our bioinformatics analysis revealed that hsa_circ_0092887 targets miR-490-5p. We hypothesized that hsa_circ_0092887 might be involved in NSCLC development and PTX-resistance via sponging miR-490-5p. Moreover, miR-490-5p was also shown to sequester the abundance of downstream oncogenes, thus exerting anti-cancer effects in multiple cancers.[17–19] Of note, there are still several miR-490-5p-targeted functional genes that have not yet been characterized. Our bioinformatics analysis suggested that miR-490-5p was targeting UBE2T. UBE2T expression has been shown to be aberrantly upregulated in NSCLC and has been linked to multiple oncogenic effects in lung cancer.[20,21] We speculated that miR-490-5p targeted UBE2T to suppress UBE2T expression, thus preventing NSCLC progression and PTX-resistance.

In the current study, we aimed to assess the expression of hsa_circ_0092887 in NSCLC with or without PTX resistance. Furthermore, we scrutinized the function of hsa_circ_0092887 in PTX-treated NSCLC to observe its role on PTX-resistance. This study aimed to provide additional biomarkers for NSCLC management and PTX therapies.

2 | MATERIALS AND METHODS

2.1 | Tissue samples

NSCLC tumor samples (n = 50) and neighboring normal samples (n = 50) were removed from patients who received PTX-based chemotherapy and surgical operation at Wuhan Hospital of Traditional Chinese Medicine. All samples were frozen and kept at a temperature of −80°C. According to the therapeutic outcomes as per the National Comprehensive Cancer Network guidelines, tumor samples were divided into PTX-resistant samples (n = 20) and PTX-sensitive samples (n = 30). Informed consent was received from all patients enrolled in this study. A permission was obtained from Wuhan Hospital of Traditional Chinese Medicine for the conduct of this study. The clinical characteristic of patients is listed in Table S1.

2.2 | Cell lines and induction of paclitaxel resistance

Human embryo lung cells (MRC5) purchased from Procell were used as non-cancer controls and cultivated in DMEM (Procell) containing 10% FBS (Procell). H1299 and A549 (NSCLC cells) bought from Procell were, respectively, cultured in F-12K medium (Procell) or RPMI1640 medium (Procell) containing 10% FBS. To generate PTX-resistant NSCLC cell lines, H1299 and A549 cells were exposed to the rising PTX concentration (from 0.1 μM to 0.5 μM; Sigma) as previously described.[22] Finally, A549/PTX and H1299/PTX cells were cultured in the corresponding culture medium containing 0.5 μM PTX to maintain PTX resistance.

2.3 | RT-qPCR

RNA samples were extracted by means of a TRIZOL reagent (Invitrogen). Afterwards, PrimeScript RT-PCR Kit (Takara) was used for the cDNA synthesis of circRNA or mRNA, and miScript II RT kit (Qiagen) was used for the cDNA synthesis of miRNAs. Nest, TB Green SYBR Mixture (Takara) was used to conduct qPCR reaction on QuantStudio 6 System (ABI). Relative expression of hsa_circ_0092887 and UBE2T mRNA was normalized by GAPDH, and was U6 was implemented to normalize the expression of miR-490-5p. The calculated method used here was $2^{-\Delta\Delta C_t}$ method. Table 1 shows the primer sequences.

2.4 | RNase R assay

A549 and H1299 cells-derived RNA samples were processed with RNase R (2 U/μg; Biovision) for 15 min at a temperature of 37°C. Subsequently, the treated RNA was subject to transcription into cDNA and designed for RT-qPCR assay.

2.5 | Subcellular location

RNA from cytoplasmic part or nuclear part of A549 and H1299 cells was isolated by mean of the commercial PARIS kit (Invitrogen). RT-qPCR revealed the presence of hsa_circ_0092887 in many parts of the body.

2.6 | Cell transfection

Small-interference-RNA specific for hsa_circ_0092887 (si-circ) or UBE2T (si-UBE2T) and si-NC were produced by Genechem. MiR-490-5p mimics (miR-490-5p), miR-490-5p inhibitors (inhibitor), along with their controls (miR-NC and inhibitor-NC) were gained from Ribobio located in Guangzhou. The experimental cells were administered with various transfections by mean of Lipofectamine™ 3000 (Invitrogen). After 24 h transfection, cells were collected to examine transfection efficiency using western blotting or RT-qPCR.

2.7 | CCK-8 assay

Cells with several treatments were cultured in 96-well plates (5×10^3 cells/well) and then cultured for the specified time, including 0, 24, 48, and 72 h. Following cell culture, 10 μl CCK-8 reagent (Sigma) was added to each well for an additional 2 h. The OD values at wavelength 450 nm were evaluated by a microplate reader (Bio-Rad).

2.8 | Wound healing assay

Cells with various treatments were maintained in 24-well plates (5×10^4 cells/well). After cell growing at 90% convergence, we used a sterile pipette tip to scratch cell surface to create a wound. The distance of wound was recorded at 0 and 24 h, and images were taken meantime by light microscopy (Olympus).

2.9 | Xenograft tumor experiment

Short hairpin RNA (ShRNA) specific to hsa_circ_0092887 (Sh-circ) and the scrambled shRNA (Sh-NC) were obtained from Genechem and were subsequently inserted into the lentiviral particles. The lentiviruses carrying Sh-circ or Sh-NC were transduced into A549/PTX cells.

All animal experiments were carried out with the approval of the animal ethics committee of the Wuhan Hospital of Traditional Chinese Medicine. Male BALB/c nude mice (4–6 weeks old) were acquired from Vital River Laboratory Animal Company, and were disturbed in two groups (five mice per group). PTX-treated A549 cells (4×10^6 cells) stably expressing either Sh-circ or Sh-NC were subcutaneously injected into the right flank of the mice. The mice were then housed at 22°C ± 3°C in a pathogen-free environment with a relative humidity of 50% ± 15% and a 12 h:12 h light:dark cycle. The width (W) and length (L) of their tumors were measured

TABLE 1 Real-time PCR Primer synthesis list

Gene	Sequences	
circ_0092887	Forward	5'-ATCGTCATCCTCCTTCCACA-3'
	Reverse	5'-CACTTCCTCTGGGCTGTCTC-3'
miR-490-5p	Forward	5'-CATGGATCTCCAGGTGG-3'
	Reverse	5'-TGGTGTCGTGGAGTCG-3'
UBE2T	Forward	5'-CCAGGCAGCTCTTAGTGTGG-3'
	Reverse	5'-TGGCTCCACCTAATATTTCTACGA-3'
U6	Forward	5'-CTCGCTTCGGCAGCACA-3'
	Reverse	5'-AACGCTTCACGAATTTGCGT-3'
GAPDH	Forward	5'-AGAAAAACCTGCCAAATATGATGAC-3'
	Reverse	5'-TGGGTGTCGCTGTTGAAGTC-3'

and documented weekly and the tumor volumes (V) were calculated using the following formula: $V = L \times W^2 \times 0.5$. Finally, after 5 weeks, the tumors were excised from the euthanized mice and their weights were recorded.

2.10 | Western blotting

Total proteins were pull out via RIPA lysis (Beyotime) and BCA Protein Assay Kit (Beyotime), in line with the protocols. Protein samples segregated by SDS-PAGE (10%) were transferred to PVDF membranes. Membranes blocked by 5% skim-milk (at room temperature, 2 h) were subject to the primary antibody (at temperature 4°C, overnight) and matched secondary antibody (room temperature, 2 h). The information of antibodies was shown below: anti-Bax (ab32503; Abcam; 1/2000), anti-Bcl-2 (ab32124; Abcam; 1/1000), anti-UBE2T (ab179802; Abcam; 1/2000), anti-GAPDH (ab9485; Abcam; 1/2000), and goat anti-rabbit IgG (ab205718; Abcam; 1/5000). Eventually, the visible protein bands were shown using the ECL Kit (Beyotime).

2.11 | Dual-luciferase reporter assay

Hsa_circ_0092887 sequence fragments comprising the mutant-type (MUT) miR-490-5p and wild-type (WT) miR-490-5p binding sites were, respectively, synthesized and implanted into firefly luciferase gene downstream in pmirGLO vector from Promega. Similarly, UBE2T 3'UTR sequence fragments harboring WT or MUT miR-490-5p binding sites were, respectively, produced and cloned into pmirGLO vector. Cells were cultivated in 96-well plates with the co-transfection of MUT or WT luciferase reporter construct (400 ng) and miR-490-5p mimic or miR-NC (40 nM). Cells were harvested after culturing cells for 48 h, and luciferase activities were scrutinized via the Dual Luciferase Reporter Assay Kit (Promega).

2.12 | RIP assay

Ago2 protein is essential for miRNA-induced RISC. To realize whether hsa_circ_0092887 was expressed in miR-490-5p-induced RISC, RIP study was performed using the Commercial RIP Assay Kit from Millipore. In short, the lysates of A549 and H1299 cells were co-cultured with magnetic beads conjugated with anti-Ago2 or anti-IgG. Then, we isolated RNA samples from beads and detected the expression of hsa_circ_0092887 using RT-qPCR.

2.13 | Statistical analysis

In this investigation, three separate biological studies were included, and GraphPad Prism 7 (GraphPad) was used for data processing. Student's *t* test or analysis of variance were applied to analyze the difference in diverse groups. Data were displayed as mean ± standard deviation. Pearson's correlation analysis was applied to scrutinize the association among miR-490-5p expression and hsa_circ_0092887 expression or UBE2T expression. $p < 0.05$ was known as a substantial difference.

3 | RESULTS

3.1 | Hsa_circ_0092887 was richly expressed in PTX-resistant tumor samples and cells

Hsa_circ_0092887 was produced by back-splicing from the exon7-exon12 regions of DHTKD1 mRNA (NM_018706), with 995 bp in length (Figure 1A). Hsa_circ_0092887 expression was found to be significantly high in tumor samples when compared with normal tissues, and it was also shown to be elevated in PTX-resistant tumor samples when compared with PTX-sensitive tumor samples (Figure 1B). Moreover, the hsa_circ_0092887 expression was associated with TNM stage and paclitaxel therapy (Table S1). In addition, hsa_circ_0092887 expression was heightened in H1299 cells and A549 cells than in MRC5 cells, and its expression was noticeably higher in PTX-resistant H1299 cells and A549 cells, corresponding to their parental cells (Figure 1C). RNase R had no effect on hsa_circ_0092887 expression, while it significantly reduced DHTKD1 expression (Figure 1D), suggesting the existence of hsa_circ_0092887. Moreover, we observed that hsa_circ_0092887 was mainly localized in the cytoplasm but not in the nucleus of NSCLC cells (Figure 1E). These results mainly illustrated that the aberrant upregulation of hsa_circ_0092887 in NSCLC might be associated with PTX-resistance.

3.2 | Silencing hsa_circ_0092887 repressed PTX-resistance in NSCLC in vitro as well as inhibited tumor formation in vivo

A549, A549/PTX, H1299 and H1299/PTX cells were administered with various PTX concentrations (from 0.05 to 12.8 μM) to monitor their IC50 to PTX. The PTX-resistant IC50 value in A549 cells was strikingly elevated than that of A549 cells, and PTX-resistant IC50 value in H1299 cells was strikingly higher comparing to H1299 cells (Figure 2A). Then, we assayed the how hsa_circ_0092887 effect functionally in NSCLC. The expression of hsa_circ_0092887 was knocked down in PTX-treated H1299 cells and A549 cells by si-circ transfection (Figure 2B). Silencing hsa_circ_0092887 in PTX-treated H1299 and A549 cells resulted in significantly reduced cell proliferation, particularly 72 h post transfection, when compared with si-NC-transfected cells (Figure 2C). Similarly, PTX-treated A549 and H1299 cells with hsa_circ_0092887 expression depletion exhibited repressive cell migratory capacity (Figure 2D). In addition, Bax expression was considerably reinforced, while Bcl-2 expression was considerably diminished in PTX-treated A549 and H1299 cells after hsa_circ_0092887 depletion (Figure 2E). The in vivo assay

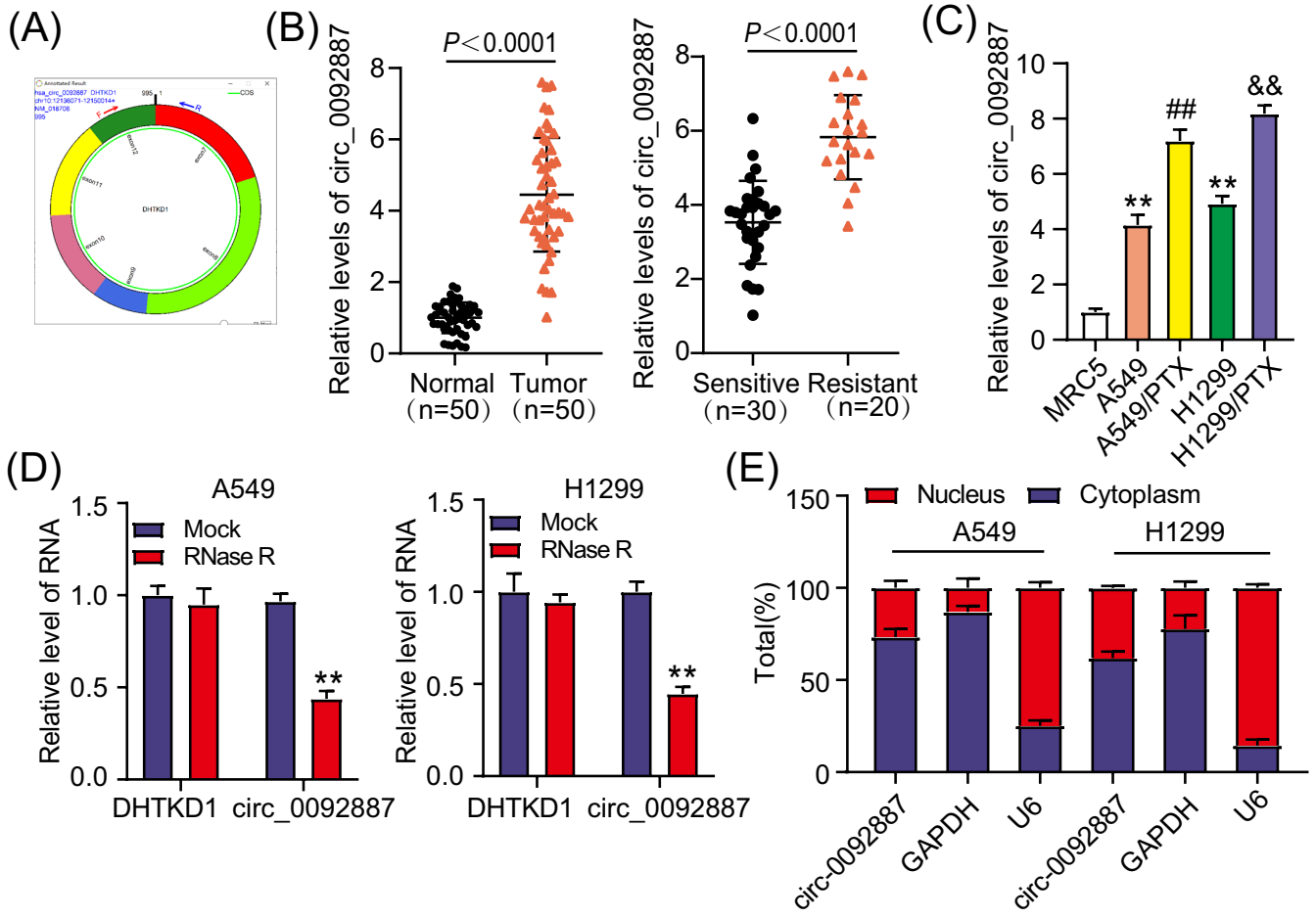

FIGURE 1 Hsa_circ_0092887 showed higher expression in PTX-resistant NSCLC tumor tissues and cells. (A) The formation and structure of hsa_circ_0092887; (B) Relative hsa_circ_0092887 expression in tumor samples and normal samples, and relative expression of hsa_circ_0092887 in PTX-resistant and PTX-sensitive tumor tissues were checked by RT-qPCR. (C) Hsa_circ_0092887 expression in MRC5, A549, H1299, and PTX-resistant A549 and H1299 cells was checked by RT-qPCR, $^{**}p<0.01$ relative to MRC5; $^{\#\#}p<0.01$ relative to A549; $^{\&\&}p<0.01$ relative to H1299. (D) The presence of hsa_circ_0092887 was ensured using RNase R, $^{**}p<0.01$ relative to Mock. (E) Subcellular location showed the site of hsa_circ_0092887 in cytoplasm and nucleus.

further validated our findings as silencing hsa_circ_0092887 significantly reduced the size, volume, and weight of tumor tissue in nude mice (Figure 2F–H). Collectively, these results suggested that hsa_circ_0092887 acts as an oncogene in NSCLC, and that silencing it decreased PTX-resistance and produced anti-cancer effects in PTX-treated NSCLC.

3.3 | MiR-490-5p was a downstream target of hsa_circ_0092887

Our bioinformatics analysis (circular RNA Interactome) showed that hsa_circ_0092887 possessed a special binding site with miR-490-5p (Figure 3A). We further observed that luciferase activities were greatly impaired in cells containing miR-490-5p and WT- hsa_circ_0092887 vector transfections, while luciferase activities were hardly affected in cells containing miR-490-5p and MUT- hsa_circ_0092887 vector transfections (Figure 3B). In addition, high abundance of hsa_circ_0092887 and miR-490-5p was captured by anti-Ago2, in comparison with anti-IgG, through RIP assay (Figure 3C). The miR-490-5p expression was significantly lower in the tumor samples when compared with normal samples, as well as its expression was notably weakened in PTX-resistant tumor samples when compared with PTX-sensitive samples (Figure 3D). Furthermore, miR-490-5p abundance was markedly declined in H1299 and A549 cells when compared with MRC5 cells, and it was much lower in H1299/PTX cells and A549/PTX cells when compared with their respective parental cells (Figure 3E). Additionally, miR-490-5p expression in tumor samples showed a negative association with hsa_circ_0092887 expression (Figure 3F). The results verified the binding of hsa_circ_0092887 to miR-490-5p.

3.4 | Hsa_circ_0092887 silencing repressed PTX-resistance in NSCLC cells via upregulating miR-490-5p

PTX-treated H1299 and A549 cells were transfected with si-NC, inhibitor-NC, inhibitor, si-circ, or si-circ+inhibitor. Subsequent expression analysis demonstrated that miR-490-5p was noticeably

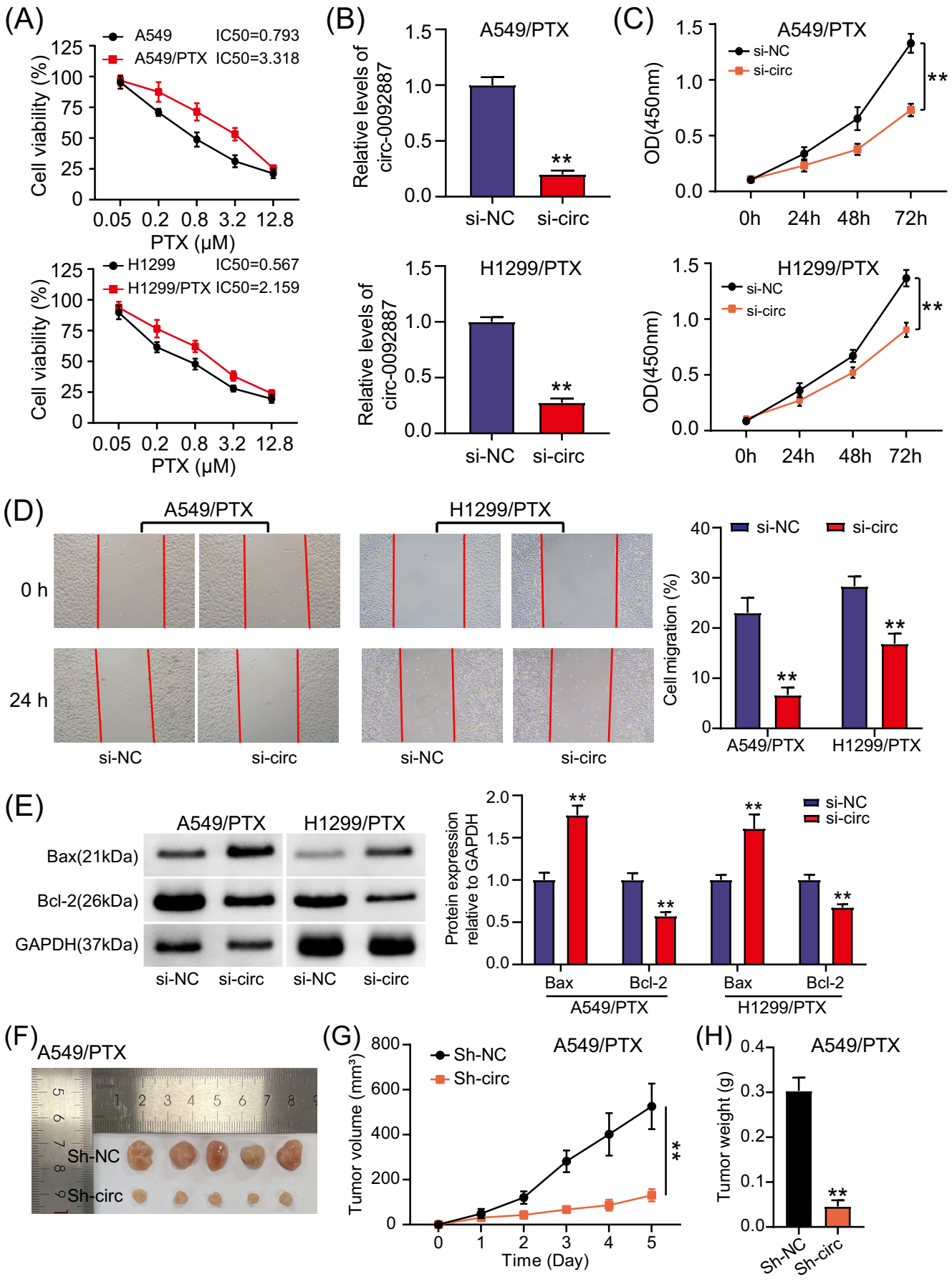
(A)
A549 IC50=0.793
A549/PTX IC50=3.318
Cell viability (%)
PTX (μM)
H1299 IC50=0.567
H1299/PTX IC50=2.159
(B)
A549/PTX
Relative levels of circ-0092887
si-NC
si-circ
H1299/PTX
(C)
A549/PTX
OD(450nm)
si-NC
si-circ
0h 24h 48h 72h
H1299/PTX
(D)
A549/PTX
H1299/PTX
0 h
24 h
si-NC
si-circ
Cell migration (%)
(E)
Bax(21kDa)
Bcl-2(26kDa)
GAPDH(37kDa)
Protein expression relative to GAPDH
Bax
Bcl-2
(F)
A549/PTX
Sh-NC
Sh-circ
(G)
A549/PTX
Sh-NC
Sh-circ
Tumor volume (mm³)
Time (Day)
(H)
A549/PTX
Tumor weight (g)

FIGURE 2 Hsa_circ_0092887 downregulation repressed PTX-resistance in NSCLC in vitro as well as inhibited tumor formation in vivo. (A) The IC50 values of H1299/PTX, A549, A549/PTX, and H1299 cells were checked using CCK-8 assay. (B) The inhibitory efficiency of si-circ on hsa_circ_0092887 expression was ascertained by RT-qPCR. (C) The outcome of hsa_circ_0092887 downregulation on cell proliferation was determined by CCK-8 assay. (D) The effect of hsa_circ_0092887 downregulation on cell migration was determined by wound healing assay. (E) The protein levels of Bax and Bcl-2 in si-circ- or si-NC-transfected cells were determined by western blotting. $^{**}p<0.01$ relative to si-NC. (F) Tumor size between Sh-NC and Sh-circ groups. (G) Tumor volumes from the Sh-NC and Sh-circ groups were measured every week. (H) After 5 weeks, the mice were sacrificed and tumor weights were evaluated in both the groups. $^{**}p<0.01$ vs. Sh-NC.

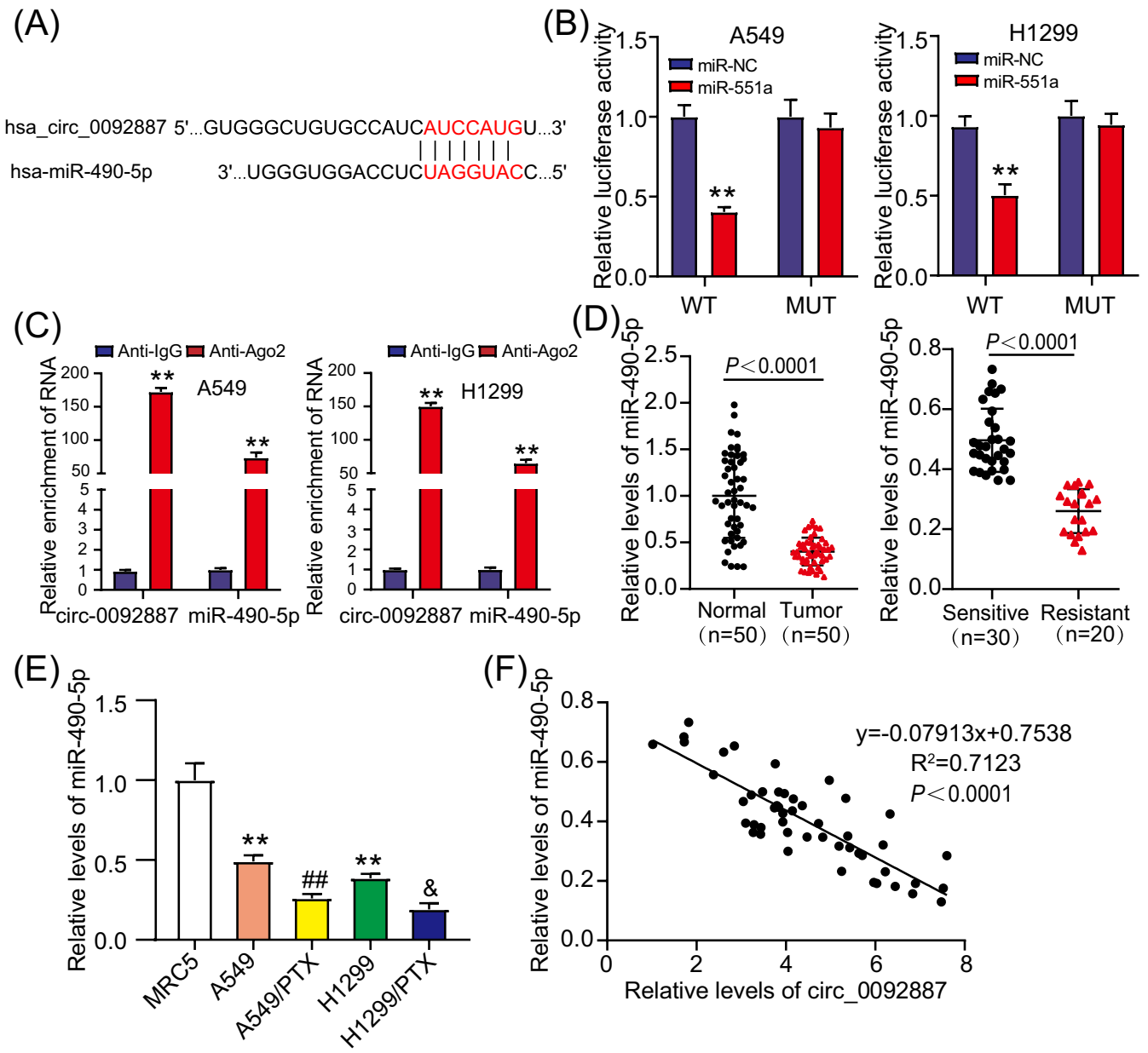

FIGURE 3 Hsa_circ_0092887 directly targeted miR-490-5p. (A) Hsa_circ_0092887 targeting miR-490-5p was predicted by circinteractome (https://circinteractome.nia.nih.gov/). (B) The predicted binding site among hsa_circ_0092887 and miR-490-5p was verified by dual-luciferase reporter study, $^{**}p<0.01$ relating miR-NC. (C) The binding of hsa_circ_0092887 to miR-490-5p was verified by RIP study, $^{**}p<0.01$ proportionate to Anti-IgG. (D) Relative expression of miR-490-5p in tumor samples and normal samples, and relative expression of miR-490-5p in PTX-resistant and PTX-sensitive tumor samples were checked by RT-qPCR. (E) Relative expression of miR-490-5p in MRC5, A549, H1299, A549/PTX, and H1299/PTX cells, $^{**}p<0.01$ proportionate to MRC5; $^{\#\#}p<0.01$ proportionate to A549; $^{\&}p<0.01$ proportionate to H1299. (F) The association among miR-490-5p expression and hsa_circ_0092887 expression in tumor samples was tested using Pearson's correlation analysis.

heightened in si-circ-transfected NSCLC cells but reduced in miR-490-5p inhibitor-transfected cells, and the enhanced expression of miR-490-5p induced by si-circ was considerably repressed by miR-490-5p inhibitor co-transfection (Figure 4A). In function, miR-490-5p inhibition aggravated the migration and proliferation of PTX-treated NSCLC cells, and hsa_circ_0092887 knockdown-mediated

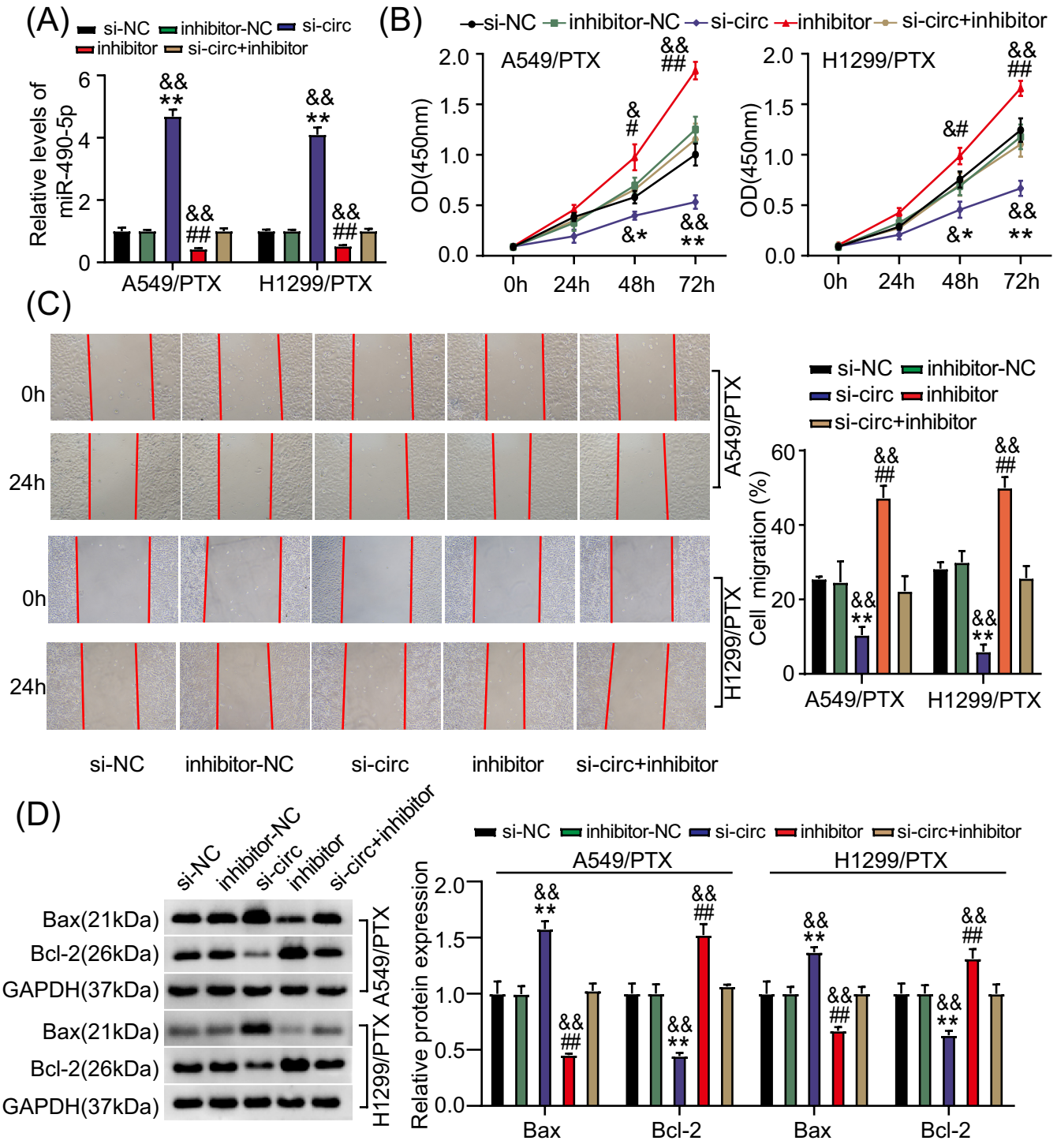

FIGURE 4 MiR-490-5p inhibition inverted the inhibitory outcomes of hsa_circ_0092887 downregulation in PTX-resistant NSCLC cells. (A–D) H1299 as well as A549 cells treated with PTX were transfected with si-NC, inhibitor-NC, si-circ, inhibitor, or si-circ + inhibitor. (A) MiR-490-5p expression in these cells was scrutinized by RT-qPCR. (B) Cell proliferation in these cells was examined by CCK-8 assay. (C) By using a wound healing test, cell migration in these cells was studied. (D) The protein levels of Bax and Bcl-2 in these cells, examined by western blotting analysis. $^{*}p < 0.05$, $^{**}p < 0.01$ corresponding to si-NC; $^{\#}p < 0.05$, $^{\#\#}p < 0.01$ corresponding to inhibitor-NC; $^{\&}p < 0.05$, $^{\&\&}p < 0.01$ corresponding to si-circ + inhibitor

suppression of proliferation and migration was mostly overturned by miR-490-5p downregulation (Figure 4B,C). Additionally, miR-490-5p downregulation impaired Bax expression and reinforced Bcl-2 expression in PTX-treated NSCLC cells, and hsa_circ_0092887 depletion-induced Bax upregulation and Bcl-2 downregulation were considerably reversed by additional miR-490-5p downregulation (Figure 4D). These findings illustrated that hsa_circ_0092887 silencing repressed PTX-resistance in NSCLC cells via upregulating miR-490-5p.

3.5 | UBE2T was a downstream target of miR-490-5p

TargetScan predicted that miR-490-5p possessed a special binding site with UBE2T 3'UTR (Figure 5A). Next, the decreased luciferase activities were observed in the experimental cells with miR-490-5p mimic and UBE2T-WT vector co-transfection (Figure 5B). The expression of UBE2T mRNA was remarkably elevated in tumor samples as well as in PTX-resistance tumor samples when compared with their corresponding controls (Figure 5C). Furthermore, UBE2T expression was significantly higher in A549 and H1299 cells compared with MRC5 cells, and its expression was also markedly higher in H1299/PTX cells and A549/PTX cells in comparison to their parental cells (Figure 5D). Interestingly, miR-490-5p expression in tumor samples was inversely linked with expression of UBE2T (Figure 5E). These results showed that UBE2T was a downstream target of hsa_circ_0092887/miR-490-5p axis.

3.6 | The anti-cancer effect of UBE2T knockdown in PTX-treated NSCLC cells was alleviated by miR-490-5p downregulation

PTX-treated NSCLC cells were transfected with si-NC, inhibitor-NC, si-UBE2T, inhibitor, or si-UBE2T + inhibitor. We detected that UBE2T expression was distinctly low in si-UBE2T-transfected cells but strengthened in miR-490-5p inhibitor-transfected cells, and UBE2T expression was markedly restored by si-UBE2T + miR-490-5p inhibitor transfection in NSCLC cells when compared with si-UBE2T (Figure 6A). In function, UBE2T downregulation markedly restrained the proliferative and migratory capacities of PTX-treated NSCLC cells, while addition of miR-490-5p inhibition partially recovered the inhibited proliferative and migratory capacities (Figure 6B,C). Moreover, UBE2T downregulation significantly enhanced Bax expression and weakened Bcl-2 expression, while UBE2T downregulation-induced Bax upregulation and Bcl-2 downregulation were largely inverted by miR-490-5p inhibition (Figure 6D). Collectively, these results indicated that miR-490-5p knockdown strengthened the UBE2T expression and thus aggravated the malignant behaviors of PTX-treated cells.

4 | DISCUSSION

PTX remains the first-line drug for advanced or metastatic NSCLC, and drug resistance is the main challenge for therapeutic outcomes.[5] Our current study looked at the effects of hsa_circ_0092887 on PTX-resistance in NSCLC. We primarily presented that hsa_circ_0092887

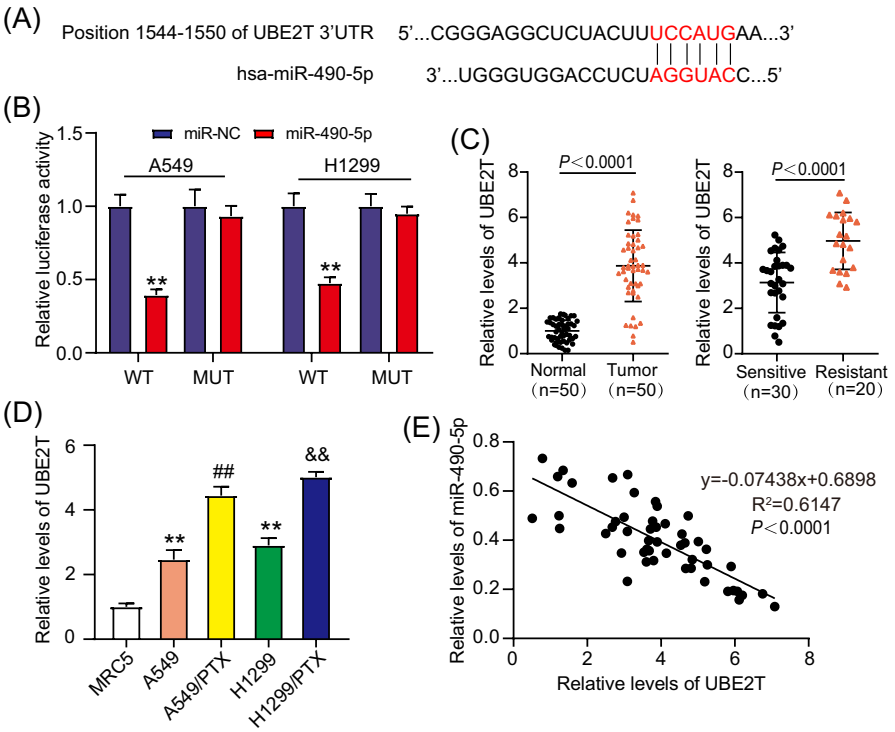

FIGURE 5 MiR-490-5p directly targeted UBE2T. (A) MiR-490-5p targeting UBE2T 3'UTR was predicted by TargetScan (http://www.targetscan.org/vert_72/). (B) The predicted binding site among miR-490-5p and UBE2T 3'UTR was validated by dual-luciferase reporter study, $^{**}p < 0.01$ proportionate to miR-NC. (C) Relative UBE2T expression in tumor samples and normal samples, and relative UBE2T expression in PTX-resistant and PTX-sensitive tumor samples were checked by RT-qPCR. (D) Relative UBE2T expression in A549/PTX, MRC5, H1299, A549, and H1299/PTX cells, $^{**}p < 0.01$ proportionate to MRC5; $^{\#\#}p < 0.01$ proportionate to A549; $^{\&\&}p < 0.01$ relative to H1299. (E) The association among miR-490-5p expression and UBE2T expression in tumor samples was tested via Pearson's correlation analysis.

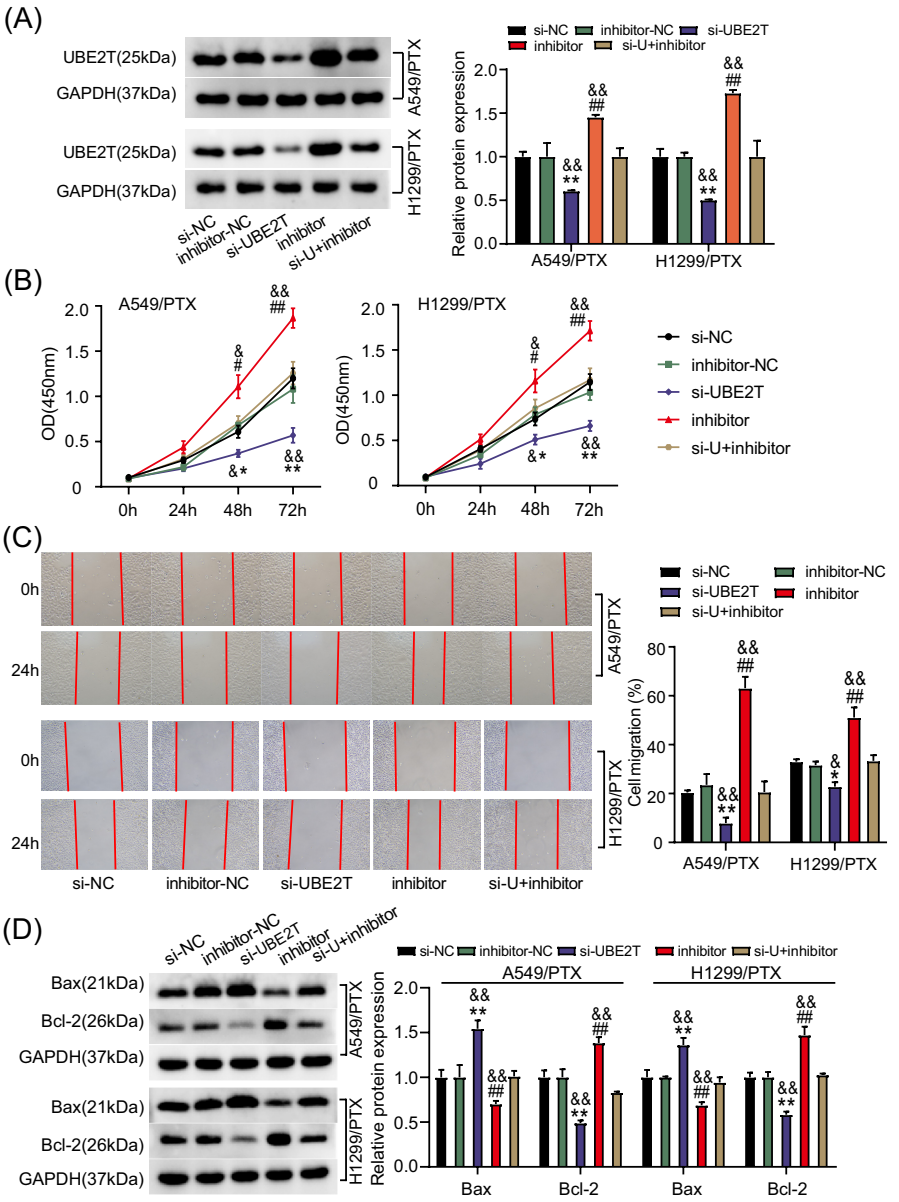

FIGURE 6 MiR-490-5p repression attenuated the inhibitory effects of UBE2T knockdown in PTX-treated NSCLC cells. (A–D) A549 and H1299 cells treated with PTX were transfected with si-NC, inhibitor-NC, si-UBE2T, inhibitor, or si-UBE2T + inhibitor. (A) The expression of UBE2T protein in these cells was examined by western blotting. (B) Cell proliferation in these cells was examined by CCK-8 assay analysis. (C) For cell migration examination, the data were taken from wound healing assay analysis. (D) The protein Bax and Bcl-2 levels in these cells were examined by western blotting. $^{*}p < 0.05$, $^{**}p < 0.01$ compared with si-NC; $^{\#}p < 0.05$, $^{\#\#}p < 0.01$ in relation to inhibitor-NC; $^{\&}p < 0.05$, $^{\&\&}p < 0.01$ relative to si-U + inhibitor; si-U representing si-UBE2T

was aberrantly upregulated in PTX-resistant tumor samples and cells. Silencing hsa_circ_0092887 repressed cell proliferation, migration and enhanced apoptosis in PTX-treated NSCLC cells. These results were supplemented by our in vivo experiment as well. We additionally demonstrated that hsa_circ_0092887 controlled the miR-490-5p/UBE2T network to respond to PTX-resistance in NSCLC, at least in part.

Nowadays, the advanced bioinformatics analysis and expression profile data identify a variety of differently expressed circRNAs in between PTX-resistant and PTX-sensitive NSCLC samples.[23] In terms of circRNA function, Li et al. discovered that circ_0002483 was poorly expressed in NSCLC samples, and ectopic circ_0002483 expression in cells and animal models impaired PTX-resistance in NSCLC.[24] In contrast, in NSCLC materials we observed rich circ_0011292 expression, particularly in NSCLC cells with PTX-resistant, and circ_0011292 silencing weakened the PTX-resistant cells IC50 to PTX.[25] In our study, we obtained hsa_circ_0092887 from GSE112214 dataset in GEO database whose results displayed that hsa_circ_0092887 was overexpressed in NSCLC tissues. Consistent with the existing data, the hsa_circ_0092887 upregulation was confirmed in our NSCLC samples and cells. Besides, we also observed enhanced expression of hsa_circ_0092887 in PTX-resistant tissue samples and cell lines relative to PTX-sensitive samples. We functionally characterized that hsa_circ_0092887 depletion restrained proliferation and migration, but accelerated cell apoptosis in NSCLC cells treated with PTX. Based on our current results, we propose that hsa_circ_0092887 overexpression confers chemoresistance to PTX in NSCLC, which might provide a therapeutic strategy for PTX-administered NSCLC.

CircRNAs harboring miRNA binding sites may bind to miRNA and thus affect the expression of downstream genes.[26] For instance, circ_0001821 deficiency reduced PTX resistance and cell aggressive phenotypes in NSCLC via miR-526b-5p upregulated-mediated

GRK5 repression.[27] Given that miR-490-5p was potentially targeted by hsa_circ_0092887, we picked miR-490-5p for additional examination and verified their interactions in NSCLC, demonstrated by the rescue impacts of miR-490-5p inhibition on the inhibited PTX-resistance caused by hsa_circ_0092887 depletion. Previous findings have shown that miR-490-5p was downregulated in hepatocellular carcinoma, and miR-490-5p restoration reduced the metastatic ability of cancer cells.[17] Likewise, miR-490-5p was also downregulated in renal cell cancer, and its restoration repressed cell proliferative, migration and invasive capacities.[19] Recent studies have also shown reduced expression of miR-490-5p in various cancers, including colon cancer, pancreatic cancer, and supraglottic laryngeal squamous cell carcinoma.[28–30] Consistently, our data demonstrated the downregulation of miR-490-5p in NSCLC, especially in PTX-resistant NSCLC samples. MiR-490-5p inhibition aggravated the migration, growth, and survival of PTX-treated NSCLC cells, suggesting that miR-490-5p deficiency conferred NSCLC PTX-resistance.

Furthermore, we recognized that UBE2T was targeted by miR-490-5p. Overexpression of UBE2T was previously reported in lung cancer and associated with poor outcomes.[20,31] UBE2T has been shown to enhance radiation resistance in NSCLC and contribute to NSCLC cell growth and epithelial–mesenchymal transition.[21] UBE2T overexpression strengthened cisplatin resistance in lung adenocarcinoma via increasing cisplatin-induced autophagy.[32] Overall, the existing evidence highlighted the oncogenic role of UBE2T in not only lung cancer but also osteosarcoma, gastric cancer, and bladder cancer.[33–35] We found that UBE2T was highly expressed in PTX-resistant NSCLC samples and cells. UBE2T silencing inhibited migration, proliferation, and survival in PTX-treated NSCLC cells, indicating that UBE2T decrease may improve PTX sensitivity. However, miR-490-5p depletion reinforced UBE2T expression and thus recovered UBE2T downregulation-reduced PTX resistance in NSCLC.

Our study demonstrated the effects of hsa_circ_0092887/miR-490-5p/UBE2T axis on PTX-resistance in NSCLC. However, the association between hsa_circ_0092887 expression and prognosis with patients was still lacking, which limited the clinical implication of hsa_circ_0092887 as a biomarker for PTX-treated NSCLC. Future work should focus on this issue.

5 | CONCLUSIONS

We found elevated hsa_circ_0092887 expression in NSCLC tissues and cells with PTX-resistance. High expression of hsa_circ_0092887 conferred NSCLC PTX-resistance via targeting the miR-490-5p/UBE2T network. We anticipate hsa_circ_0092887 to be a new biomarker in PTX-treated NSCLC, which is subject to further validation.

AUTHOR CONTRIBUTIONS

LMW performed the experiments and data analysis and did investigation. HT conceived and designed the study and found resources required. ZYZ formed the methodology. The article was transcribed by LMW. The article was reviewed and edited by ZYZ and HT. The article has been read and approved by all authors.

ACKNOWLEDGMENTS

None.

CONFLICT OF INTEREST

According to the authors, there is no conflict of interest.

DATA AVAILABILITY STATEMENT

This article contains all of the data that were created or examined during this investigation.

CONSENT TO PARTICIPATE

Each patient completed an informed consent form in writing.

CONSENT FOR PUBLICATION

Participants gave their permission for their names to be published.

ORCID

Hui Tian https://orcid.org/0000-0002-8419-5954

REFERENCES

1. Sung H, Ferlay J, Siegel RL, et al. Global cancer statistics 2020: GLOBOCAN estimates of incidence and mortality worldwide for 36 cancers in 185 countries. *CA Cancer J Clin*. 2021;71(3):209-249.
2. Zappa C, Mousa SA. Non-small cell lung cancer: current treatment and future advances. *Transl Lung Cancer*. 2016;5(3):288-300.
3. González M, Calvo V, Redondo I, Provencio M. Overall survival for early and locally advanced non-small-cell lung cancer from one institution: 2000–2017. *Clin Transl Oncol*. 2021;23(7):1325-1333.
4. Liu J, Liu X, Dong M, et al. Symptom trajectories during chemotherapy in patients with non-small cell lung cancer (NSCLC) and the function of prolonging low dose dexamethasone in promoting enhanced recovery after chemotherapy. *Thorac Cancer*. 2021;12(6):783-795.
5. Cui H, Arnst K, Miller DD, Li W. Recent advances in elucidating paclitaxel resistance mechanisms in non-small cell lung cancer and strategies to overcome drug resistance. *Curr Med Chem*. 2020;27(39):6573-6595.
6. Tang Y, Qiao G, Xu E, Xuan Y, Liao M, Yin G. Biomarkers for early diagnosis, prognosis, prediction, and recurrence monitoring of non-small cell lung cancer. *Onco Targets Ther*. 2017;10:4527-4534.
7. Xie S, Ogden A, Aneja R, Zhou J. Microtubule-binding proteins as promising biomarkers of paclitaxel sensitivity in cancer chemotherapy. *Med Res Rev*. 2016;36(2):300-312.
8. Chen B, Huang S. Circular RNA: an emerging non-coding RNA as a regulator and biomarker in cancer. *Cancer Lett*. 2018;418:41-50.
9. Li Z, Ruan Y, Zhang H, Shen Y, Li T, Xiao B. Tumor-suppressive circular RNAs: mechanisms underlying their suppression of tumor occurrence and use as therapeutic targets. *Cancer Sci*. 2019;110(12):3630-3638.
10. Lu Y, Li Z, Lin C, Zhang J, Shen Z. Translation role of circRNAs in cancers. *J Clin Lab Anal*. 2021;35(7):e23866.
11. Wang S, Zhang K, Tan S, et al. Circular RNAs in body fluids as cancer biomarkers: the new frontier of liquid biopsies. *Mol Cancer*. 2021;20(1):13.
12. Li J, Fan R, Xiao H. Circ_ZFR contributes to the paclitaxel resistance and progression of non-small cell lung cancer by

upregulating KPNA4 through sponging miR-195-5p. *Cancer Cell Int*. 2021;21(1):15.
13. Xu J, Ni L, Zhao F, et al. Overexpression of hsa_circ_0002874 promotes resistance of non-small cell lung cancer to paclitaxel by modulating miR-1273f/MDM2/p53 pathway. *Aging*. 2021;13(4):5986-6009.
14. Jiang MM, Mai ZT, Wan SZ, et al. Microarray profiles reveal that circular RNA hsa_circ_0007385 functions as an oncogene in non-small cell lung cancer tumorigenesis. *J Cancer Res Clin Oncol*. 2018;144(4):667-674.
15. Zhang S, Zeng X, Ding T, et al. Microarray profile of circular RNAs identifies hsa_circ_0014130 as a new circular RNA biomarker in non-small cell lung cancer. *Sci Rep*. 2018;8(1):2878.
16. Zhao W, Zhang Y, Zhu Y. Circular RNA circβ-catenin aggravates the malignant phenotype of non-small-cell lung cancer via encoding a peptide. *J Clin Lab Anal*. 2021;35(9):e23900.
17. Fang ZQ, Li MC, Zhang YQ, Liu XG. MiR-490-5p inhibits the metastasis of hepatocellular carcinoma by down-regulating E2F2 and ECT2. *J Cell Biochem*. 2018;119(10):8317-8324.
18. Yu Y, Cai O, Wu P, Tan S. MiR-490-5p inhibits the stemness of hepatocellular carcinoma cells by targeting ECT2. *J Cell Biochem*. 2019;120(1):967-976.
19. Chen K, Zeng J, Tang K, et al. miR-490-5p suppresses tumour growth in renal cell carcinoma through targeting PIK3CA. *Biol Cell*. 2016;108(2):41-50.
20. Hao J, Xu A, Xie X, et al. Elevated expression of UBE2T in lung cancer tumors and cell lines. *Tumour Biol*. 2008;29(3):195-203.
21. Yin H, Wang X, Zhang X, et al. UBE2T promotes radiation resistance in non-small cell lung cancer via inducing epithelial-mesenchymal transition and the ubiquitination-mediated FOXO1 degradation. *Cancer Lett*. 2020;494:121-131.
22. Sun H, Zhou X, Bao Y, Xiong G, Cui Y, Zhou H. Involvement of miR-4262 in paclitaxel resistance through the regulation of PTEN in non-small cell lung cancer. *Open Biol*. 2019;9(7):180227.
23. Xu N, Chen S, Liu Y, et al. Profiles and bioinformatics analysis of differentially expressed Circrnas in Taxol-resistant non-small cell lung cancer cells. *Cell Physiol Biochem*. 2018;48(5):2046-2060.
24. Li X, Yang B, Ren H, et al. Hsa_circ_0002483 inhibited the progression and enhanced the Taxol sensitivity of non-small cell lung cancer by targeting miR-182-5p. *Cell Death Dis*. 2019;10(12):953.
25. Guo C, Wang H, Jiang H, Qiao L, Wang X. Circ_0011292 enhances paclitaxel resistance in non-small cell lung cancer by regulating miR-379-5p/TRIM65 Axis. *Cancer Biother Radiopharm*. 2022;37(2):84-95.
26. Panda AC. Circular RNAs act as miRNA sponges. *Adv Exp Med Biol*. 2018;1087:67-79.
27. Liu Y, Li C, Liu H, Wang J. Circ_0001821 knockdown suppresses growth, metastasis, and TAX resistance of non-small-cell lung cancer cells by regulating the miR-526b-5p/GRK5 axis. *Pharmacol Res Perspect*. 2021;9(4):e00812.
28. Yang YJ, Luo S, Xu ZL. Effects of miR-490-5p targeting CDK1 on proliferation and apoptosis of colon cancer cells via ERK signaling pathway. *Eur Rev Med Pharmacol Sci*. 2022;26(6):2049-2056.
29. Xu Z, Chen Z, Peng M, et al. MicroRNA MiR-490-5p suppresses pancreatic cancer through regulating epithelial-mesenchymal transition via targeting MAGI2 antisense RNA 3. *Bioengineered*. 2022;13(2):2673-2685.
30. Wu C, Wang M, Huang Q, et al. Aberrant expression profiles and bioinformatic analysis of CAF-derived exosomal miRNAs from three moderately differentiated supraglottic LSCC patients. *J Clin Lab Anal*. 2022;36(1):e24108.
31. Perez-Peña J, Corrales-Sánchez V, Amir E, Pandiella A, Ocana A. Ubiquitin-conjugating enzyme E2T (UBE2T) and denticleless protein homolog (DTL) are linked to poor outcome in breast and lung cancers. *Sci Rep*. 2017;7(1):17530.
32. Zhu J, Ao H, Liu M, Cao K, Ma J. UBE2T promotes autophagy via the p53/AMPK/mTOR signaling pathway in lung adenocarcinoma. *J Transl Med*. 2021;19(1):374.
33. Wang Y, Leng H, Chen H, et al. Knockdown of UBE2T inhibits osteosarcoma cell proliferation, migration, and invasion by suppressing the PI3K/Akt signaling pathway. *Oncol Res*. 2016;24(5):361-369.
34. Li L, Liu J, Huang W. E2F5 promotes proliferation and invasion of gastric cancer through directly upregulating UBE2T transcription. *Dig Liver Dis*. 2021;54(7):937-945.
35. Gong YQ, Peng D, Ning XH, et al. UBE2T silencing suppresses proliferation and induces cell cycle arrest and apoptosis in bladder cancer cells. *Oncol Lett*. 2016;12(6):4485-4492.

SUPPORTING INFORMATION

Additional supporting information can be found online in the Supporting Information section at the end of this article.

How to cite this article: Wang L, Zhang Z, Tian H. Hsa_circ_0092887 targeting miR-490-5p/UBE2T promotes paclitaxel resistance in non-small cell lung cancer. *J Clin Lab Anal*. 2023;37:e24781. doi:10.1002/jcla.24781